

EFFECT OF DEPOLYMERIZATION ON ELECTROCHEMICAL PROPERTIES OF NANO-SILICON POWDERS

W. LI*, L. ZHOU, J. LIU

Central Academe, Shanghai Electric Group Co., Ltd. Shanghai 200070, China

In order to limit the volume expansion of silicon in the process of lithiation/delithiation and achieve the ideal coating of silicon materials, the silicon needs to be depolymerized and dispersed. In this paper nano-silicon powders were depolymerized by ball milling and mechanical grinding, the effects of different depolymerization methods and different depolymerization time on nano-silicon powders were studied. The results showed that the particle size of nano-silicon powders decreased significantly after 30 min of ball milling and the D50 decreased from 4.9 μm to 0.041 μm . Meanwhile the morphology and specific surface area of the nano-silicon powders were greatly changed by ball milling. Both the initial charge capacity and the initial coulombic efficiency decreased obviously at 0.1 C rate. After mechanical grinded for 1 min, the particle size of D50 decreased from 4.9 μm to 1.77 μm , the morphology had no significantly changed and the specific surface area increased slightly. The initial coulombic efficiency at 0.1 C rate increased from 91.65% to 92.06%, and the capacity retention after 22 cycles with different rates increased from 75.02% to 81.3%. The results of XRD and Infrared spectrum showed that a small amount of nano-silicon powders were oxidized into SiO_x in the process of depolymerization, and the degree of oxidation was increased with depolymerization time.

(Received December 5, 2019; Accepted April 22, 2020)

Keywords: Lithium Ion battery, Anode material, Nano-silicon, Ball milling, Mechanical grinding

1. Introduction

On April 25, 2017, the Ministry of Industry and Information Technology of the People's Republic of China (MIIT), the National Development and Reform Commission (NDRC) and the Ministry of Science and Technology (MOST) issued <The medium and long-term development plan for the automobile industry>, which clearly stated that the specific energy of single cell should reach more than 300 Wh/kg by 2020, the specific energy of the system should strive to reach 260 Wh/kg by 2020, and the specific energy of the power battery system should reach 350 Wh/kg by 2025. In order to meet the above needs, it is urgent to develop anode and cathode materials with high energy density to improve the energy density of single cell. On December 26, 2018, the MIIT released <The first batch of demonstration and guidance catalogue for the application of key new materials (edition 2018)>, which focused on the development of silicon

* Corresponding author: 361377505@qq.com

carbon anode materials as new energy materials to solve the problem of insufficient driving range of new energy vehicles.

At present, most of the anode materials of lithium ion batteries are made of graphite, which has theoretical capacity of 372 mAh/g at room temperature, cannot meet growing capacity demands for next lithium ion batteries. While silicon has the theoretical capacity of 3579 mAh/g, low lithium insertion voltage (~0.4 V versus Li^+/Li) and friendly environment. It is regarded as one of the most promising alternative candidates for next generation of high-energy density anode materials^[1-2]. However, silicon undergoes a huge volume change (around 280%) during the lithiation/delithiation process, leading to severe pulverization which directly generates serious decline in electrochemical properties^[3]. Nanometer scale, porous, alloying, surface structure optimization design, development of new silicon-based binder and electrolyte additives can effectively alleviate the expansion of silicon^[4-12]. Up to now, the most promising commercialization is carbon coating technology, which can cover the surface of silicon with a layer of carbon materials, inhibit the expansion of silicon, and improve the conductivity of silicon at the same time^[13-15]. In order to achieve the ideal coating of silicon materials, the silicon needs to be depolymerized to achieve the single particle coating, which can achieve the maximum inhibition of silicon expansion. Therefore, the effect and manner of depolymerization have a direct impact on the electrochemical properties of silicon. In this paper, ball milling and mechanical grinding were used to depolymerize nano-silicon powders.

2. Experimental

2.1. Materials synthesis

Commercial nano-silicon powders (99.9%, ST-NANO material technology Co., Ltd., China) marked as si-0 min were used as raw and dispersed in ethanol solution for mass fraction of 5%. Wet ball milling depolymerization was carried out for 30 min and 60 min using ball miller (0.3L, Nalong, China) with a rotation speed of 2200 rpm, and the samples were drying under the condition of N_2 atmosphere at 90°C for 2 h, respectively denoted as si-30 min and si-60 min. The ball-to-powder mass ratio was 15:1, and the dimension of ZrO_2 balls was 0.1 mm. 8 g nano-silicon powders were put into the mechanical grinder (M20, IKA, Germany) at a speed of 20000 rpm for 1 min, 5 min and 10 min, respectively marked as si-1 min, si-5 min and si-10 min. The grinder was shut down every 30 s to mix the nano-silicon powders again.

2.2. Materials characterization

Particle size distribution was measured by the laser scattering method using a laser diffraction particle size analyzer (Malvern 3000). Specific surface area of the samples were calculated using the Brunauer-Emmett-Teller (BET) mode and performed on Gemini VII (Micromeritics Instrument Corp., USA). Infrared spectrum was tested by Nicolet IS5 (Thermo Fisher Scientific Corp., USA). The morphology of nano-silicon powders were observed by field emission scanning electron microscope (FE-SEM, SUPRA55, Zeiss). The crystalline structures of samples were measured by X-ray diffraction (XRD, D8 Advance, Bruker) with $\text{Cu K}\alpha$ radiation at a scanning rate of 2°/min in a reflection mode over a 2θ ranging from 10° to 90°.

2.3. Electrochemical test

The working electrodes were prepared by a slurry uniformly coated onto the copper foil, including 60wt% active material, 20wt% Super P, 8wt% CMC and 12wt% SBR dissolved in deionized water. The electrodes were dried in oven at 50°C for 5 min and then in vacuum 90°C for 12 h. The mass loading of the active material on the working electrodes was $\sim 1.1 \text{ mg cm}^{-2}$. The electrochemical performances of nano-silicon powder were tested in CR2032 coin-type cells. Coin cells were assembled in a glove box full of argon (LABstar, MBRAUN Co., Ltd., China) using Li foil as the counter/reference electrode, Celgard 2400 as a separator and 1M LiPF_6 in ethylene carbonate/ dimethyl carbonate (EC/DMC, 1:1 by volume) with 1 wt% vinyl carbonate (VC) and 10 wt% fluoroethylene carbonate (FEC) additives as the electrolyte. Before the test, coin cells were placed at room temperature for 12 h. LAND 2013A battery tester was used for galvanostatic measurements. The charge and discharge procedures in this paper as followed: 0.1C charge and discharge cycle was set as gradient discharge 0.1 C to 5 mv, 0.05 C to 5 mv, 0.02 C to 5 mv, and then charge 0.1 C to 2 v. 0.5 C charge and discharge cycle was set as gradient discharge 0.5 C to 5 mv, 0.2 C to 5 mv, 0.1 C to 5 mv, 0.05 C to 5 mv, 0.02 C to 5 mv, and then charge 0.5 C to 2 v, 1 C=3200 mA/g.

3. Results and discussion

Fig. 1(a) shows the particle size distribution of nano-silicon powders at different ball milling depolymerization time. The particle size distribution at 50%, D50 is 4.19 μm , 0.041 μm and 0.0408 μm corresponding for si-0 min, si-30 min and si-60 min. The particle size of si-0 min decreased significantly after ball milling. Compared with si-30 min, the particle size distribution of si-60 min is basically unchanged in the range of 0.01 μm -0.1 μm , and the particle size distribution changes slightly at 90%, which is reduced from 0.15 μm to 0.128 μm . Figure 1(b) shows the particle size distribution of nano-silicon powders at different mechanical grinding depolymerization time. The particle size distribution of nano-silicon powders shifted negatively to the left after mechanical grinding, and D50 was 1.77 μm , 1.45 μm and 1.35 μm corresponding for si-1 min, si-5min and si-10min. There is no obviously different in D50 among of samples, so we adopt si-1min as an example of mechanical grinding to discussion in this paper. Particle size distribution of nano-silicon powders at different depolymerization time are shown in Table 1.

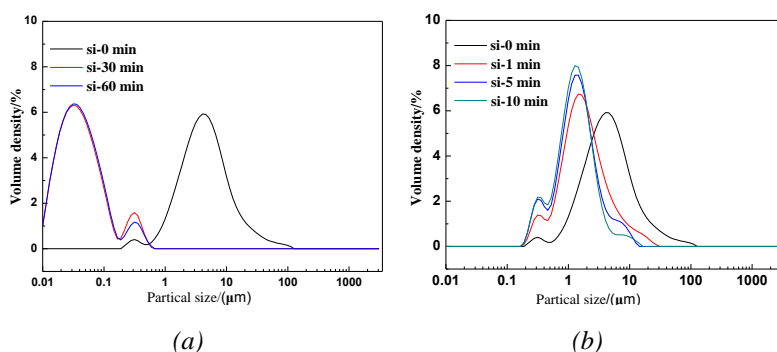


Fig. 1. (a) The particle size distribution of nano-silicon powders at different ball milling depolymerization time and (b) particle size distribution of nano-silicon powders at different mechanical grinding depolymerization time.

Table 1. Particle size distribution of nano-silicon powders at different depolymerization time.

samples	D10/ (μm)	D50/ (μm)	D90/ (μm)
0 min	1.43	4.19	13.6
30 min	0.0168	0.041	0.15
60 min	0.0168	0.0408	0.128
1 min	0.638	1.77	5.92
5 min	0.471	1.45	3.95
10 min	0.459	1.35	3.11

Fig. 2 SEM observations show that the surface morphology of si-0 min changed significantly with the ball milling depolymerization time, and the si-0 min particles changed from spheroid to irregular morphology. After the process of ball milling for 30 min and 60 min, the surface of nano-silicon powders became rough, loose and porous, accompanied by severe agglomeration. No large particles aggregation are observed in the field of si-1 min, indicating that the large particles aggregation in si-0 min have been depolymerized, and the surface morphology of si-1 min does not change significantly, which is still a spherical particles. Table 2 shows the specific surface area of nano-silicon powders at different depolymerization time. It can be concluded that the specific surface area of si-60 min increases greatly from the original 12.464 m^2/g to 233.2797 m^2/g , but increases slightly to 13.175 m^2/g of si-1 min.

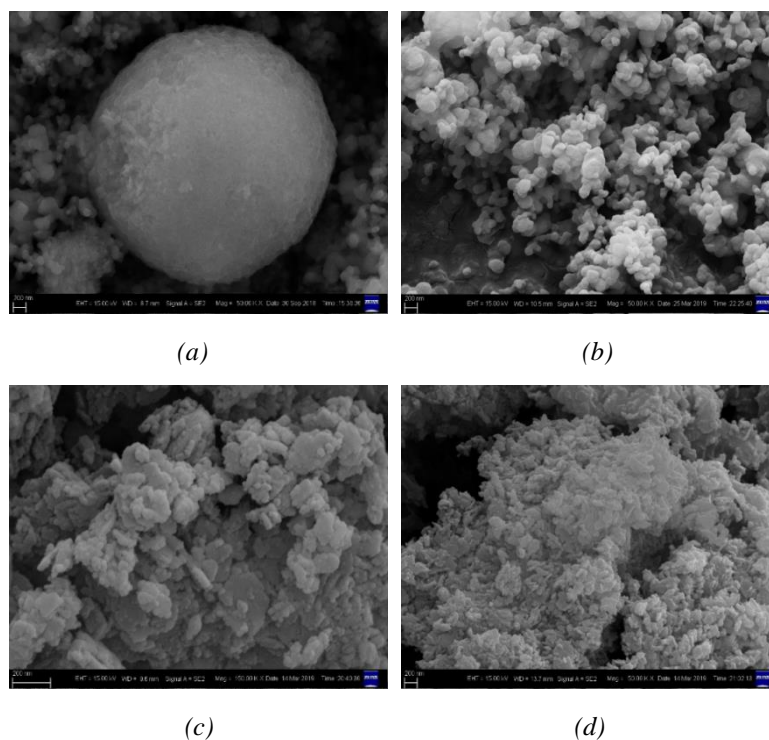


Fig. 2. SEM images of (a) si-0 min, (b) si-1 min, (c) si-30 min, (d) si-60 min

Table 2. BET surface area of nano-silicon powders at different depolymerization time.

samples	si-0 min	si-30 min	si-60 min	si-1 min
BET/(m ² /g)	12.4644	178.4427	233.2797	13.1750

Fig. 3(a) shows the XRD patterns of si-0 min and si-60 min. Si-0 min demonstrate well-defined peaks indexed to (111) at 28.381°, (220) at 47.334°, (311) at 56.188°, (400) at 69.151°, (331) at 76.551° and (422) at 88.192°. In contrast to well crystalline, the peaks of si-60 min only appear at 28.4° and 47.244°, and the peaks are obvious broader, lower and less crystalline than si-0 min. It is due to the formation of amorphous silicon and SiO_x which is due to oxygen in the air dissolved into the solution generating SiO_x in the process of ball milling. The results are consistent with infrared spectrum analysis. The peaks are accompanied by a small amount of broadening, indicating that si-0 min particles were refined. This conclusion is consistent with the particle size distribution and the results of SEM. Figure 3(b) shows the XRD of si-0 min and si-1 min. The peaks intensity of si-1 min is slightly weakened, and the characteristic peaks of si-1 min do not change significantly.

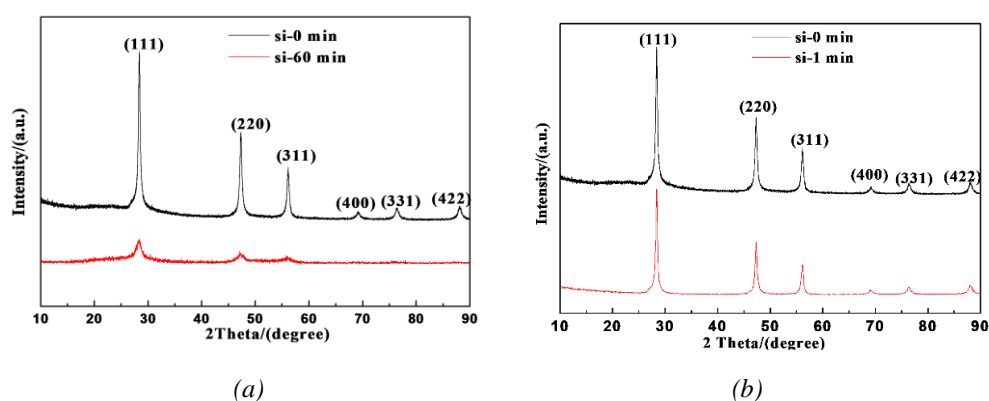


Fig. 3. (a) X-ray diffraction (XRD) of si-60 min and (b) X-ray diffraction (XRD) of si-1 min.

The surface functional groups of samples were analyzed by infrared spectrum as shown in Fig. 4(a-d). The peaks of (a-d) near 3444 cm⁻¹ and 1633 cm⁻¹ belong to O-H bond asymmetric vibration and H-O-H bending vibration respectively. It indicates si-0 min has no surface functional groups, because no other peaks are observed. The peaks near 1130 cm⁻¹, 1098 cm⁻¹ and 1065 cm⁻¹, which attribute to si-1 min, si-30 min and si-60 min respectively, are Si-O-Si bond asymmetric vibration. This may be attributed to the different valence states of silicon, resulting in different positions of absorption peaks. It can be concluded from Fig. 4(c) and Fig. 4(d) that the number of oxygen-containing functional groups of nano-silicon powders increase with depolymerization time, and oxidation degree of nano-silicon powders are increasing.

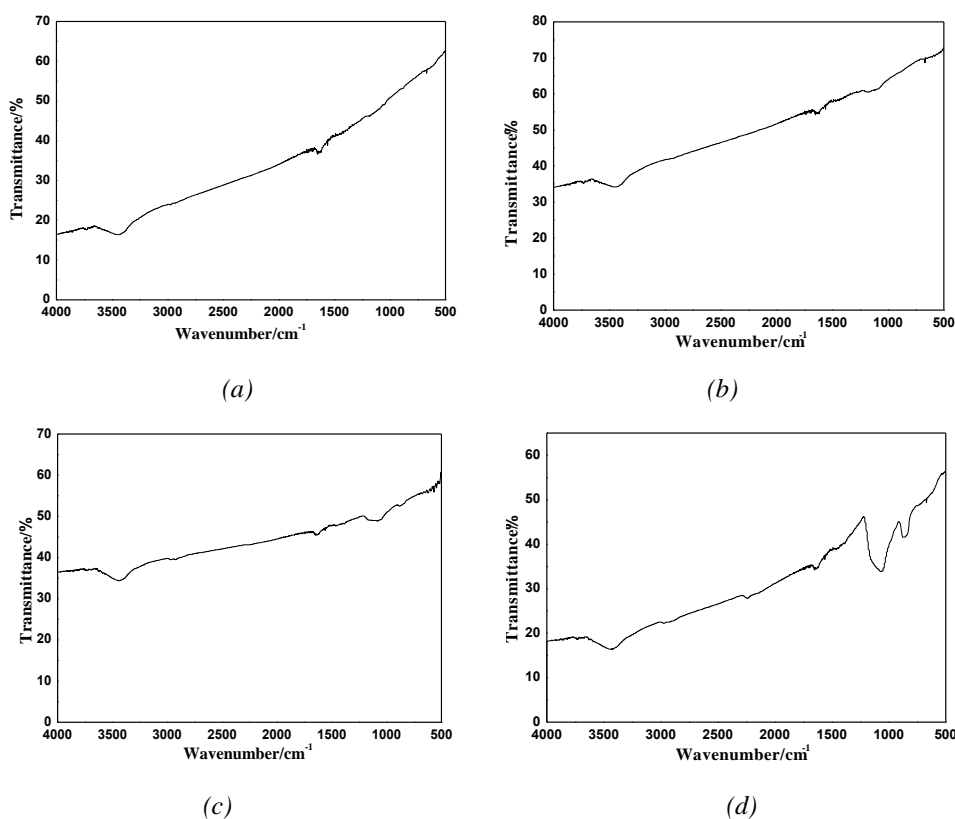


Fig. 4. Infrared spectrum of (a) si-0 min, (b) si-1 min, (c) si-30 min, (d) si-60 min

Fig. 5(a) shows the initial charge and discharge curves of si-0 min, si-30 min and si-60 min at 0.1 C rate. All samples have a small ramp between 10 mv and 1 v due to SEI formation during the first lithium insertion. The lithium insertion platform of si-0 min appears at 0.07 V, corresponding to the formation of Li_xSi alloy, and the lithium extraction platform appears at 0.4 V is the process of Li_xSi alloy delithium which generates amorphous silicon. Si-0 min has the highest initial charge capacity of 3395.6 mAh/g and the initial coulombic efficiency of 91.65%, while si-30 min and si-60 min have the initial charge capacity of 1826 mAh/g and 1584 mAh/g, and the initial coulombic efficiency of 64.48% and 57.73%, respectively. As the time of ball milling depolymerization prolonged, the initial coulombic efficiency of nano-silicon powders decreases obviously, which is caused by the sharp increase of specific surface area of nano-silicon powders after ball milling depolymerization as shown in table 2, and the sharp increase of specific surface area also consumes more lithium ions when SEI formed. Figure 5(b) shows the initial charge and discharge curves at 0.1 C of si-0 min and si-1 min. It can be seen from the figure that the polarization of si-1 min decreases, with the first charge capacity of 3369.4 mAh/g, as well as the initial coulombic efficiency of 92.06%.

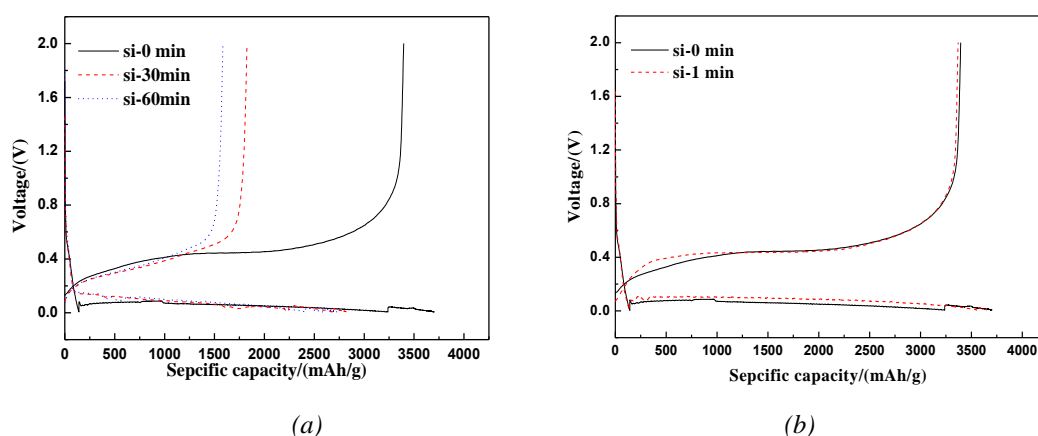


Fig. 5. (a) First charge and discharge curves of si-0 min, si-30 min and si-60 min, (b) first charge and discharge curves of si-0 min and si-1min.

The second charge and discharge curves of all samples are shown in Fig. 6 (a-d). Compared with the first cycle, in the second cycle the small slope between 10 mV and 1 V disappears, the polarization decreases, and the coulombic efficiency is significantly improved, as shown in Table 3. Si-1 min has the highest coulombic efficiency of 98.48%, indicating that a stable SEI formed during the initial charge and discharge cycle.

Table 3. Coulombic efficiency of si-0 min, si-30 min, si-60 min and si-1 min in the second cycle at different depolymerization time.

Samples	si-0 min	si-30 min	si-60 min	si-1 min
2nd coulombic efficiency / (%)	96.93	94.52	94.28	98.48

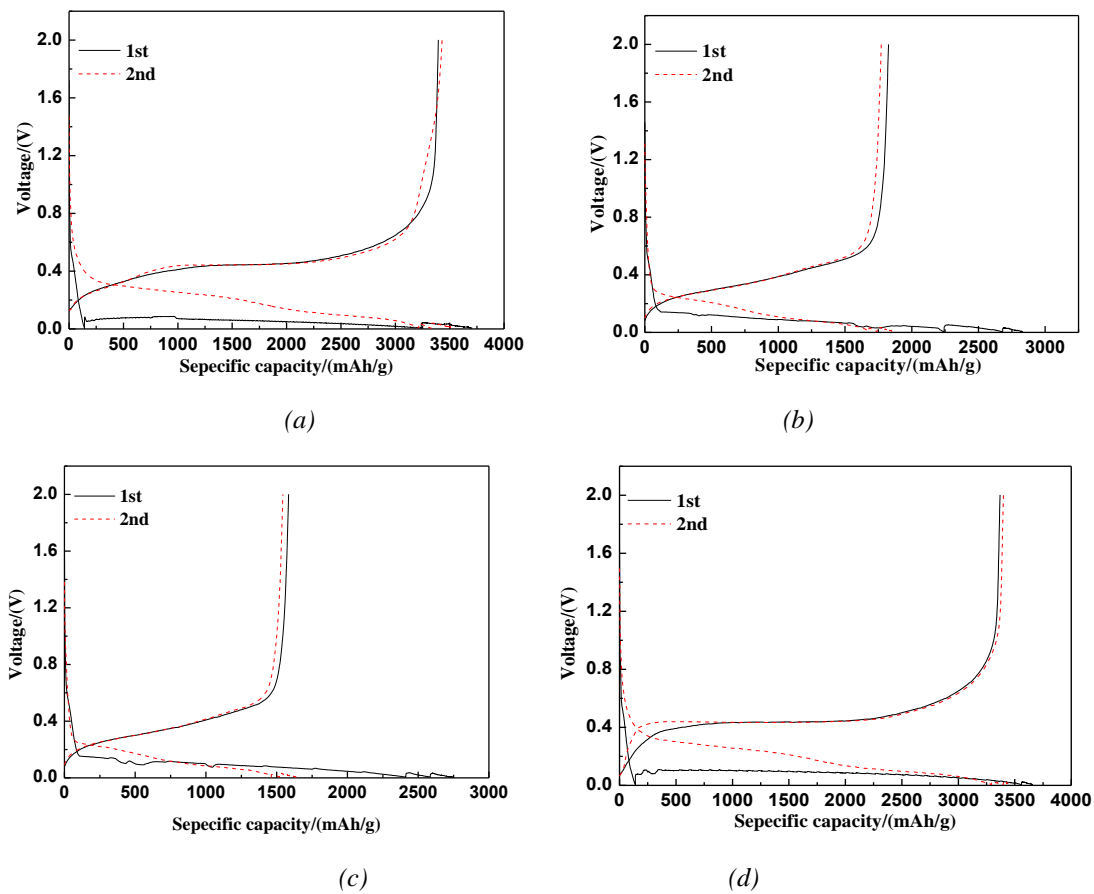


Fig. 6. Charge and discharge curves of (a) si-0 min, (b) si-30 min, (c) si-60 min and (d) si-1 min at 0.1C rate.

Fig. 7(a) shows the cycling performance at different rates of si-0 min, si-30 min and si-60 min. Three samples undergo 6 cycles at 0.1 C and 16 cycles at 0.5 C. Capacity retention of si-0 min, si-30 min, si-60 min could reach 91.27%, 91.17% and 85.51%, respectively after initial 6 cycles at 0.1 C. And the corresponding capacity retention of si-0 min, si-30 min, si-60 min is 75.02%, 66.36% and 71.18%, respectively after 16 cycles at 0.5 C. These results indicate that si-0 min has the best cycling performance. Fig. 7(b) shows the cycling performance at different rates of si-0 min and si-1 min. Obviously cycling performance of si-1 min is better than si-0 min by capacity retention of 99.48% after initial 6 cycles at 0.1 C and 81.3% after 16 cycles at 0.5 C.

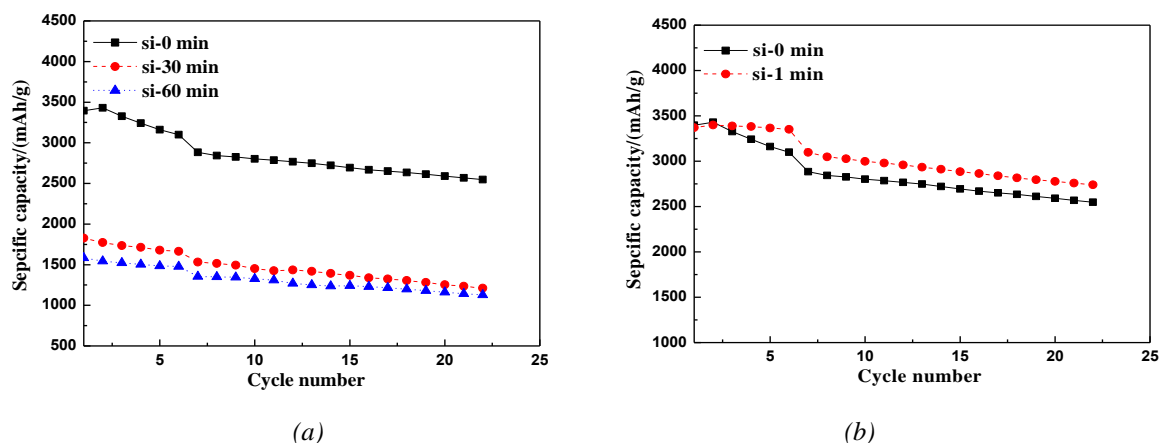


Fig. 7. (a) Cycling curves at different rates of si-0 min, si-30 min and si-60 min, (b) cycling curves at different rates of si-0 min and si-1 min.

4. Conclusions

After depolymerized by ball milling, the particle size of nano-silicon powders decreased greatly, the morphology of particles changed from spheroid to irregular, but the specific surface area of nano-silicon powders increased obviously. The formation of SEI consumes a amount of lithium ions in the first charge and discharge process, and the consuming results in the decrease of initial coulombic efficiency. Si-30 min and si-60 min have the initial charge capacity of 1826 mAh/g and 1584 mAh/g, and the initial coulombic efficiency of 64.48% and 57.73% at 0.1 C, respectively, which is far less than 3395.6 mAh/g and 91.65% of si-0 min. After mechanical grinded for 1min, the particle size of nano-silicon powders decreased slightly, the specific surface area increased slightly, but the morphology had no significantly changed. After the first charge and discharge at 0.1 C stable SEI formed, which has good electrochemical performance with initial charge capacity of 3369.4 mAh/g, as well as the initial coulombic efficiency of 92.06%. Cycling performance of si-1 min is better than si-0 min by capacity retention of 99.48% after initial 6 cycles at 0.1 C and 81.3% after 16 cycles at 0.5 C.

References

- [1] Huajun Tian, Xiaojian Tan, Fengxia Xin, Chunsheng Wang, Weiqiang Han, *Nano Energy* **11**, 490 (2015).
- [2] Naoki Nitta, Feixiang Wu, Jung Tae Lee, Gleb Yushin, *Materials today* **18**(5), 252 (2015).
- [3] M. N. Obrovac, L. J. Krause, *Journal of the Electrochemical Society* **154**(2), A103 (2007).
- [4] J. R. Szczech, S. Jin, *Energy & Environmental Science* **4**(1), 56 (2011).
- [5] Mi-Hee Park, Min Gyu Kim, Jaebum Joo, Kitae Kim, Jeyoung Kim, Soonho Ahn, Yi Cui, Jaephil Cho, *Nano letters* **9**(11), 3844 (2009).
- [6] Bo Li, Rongrong Qi, Jiantao Zai, Feihu Du, Chi Xue, Ying Jin, Chengyou Jin, Zifeng Ma, Xuefeng Qian, *Small* **12**(38), 5281 (2016).
- [7] Haiping Jia, Jianming Zheng, Junhua Song, Langli Luo, Ran Yia, Luis Esteveza,

- Wengao Zhao, Rajankumar, Patela, Xiaolin Lia, Ji-Guang Zhang, *Nano energy* **50**, 589 (2018).
- [8] Chao Xu, Fredrik Lindgren, Bertrand Philippe, Mihaela Gorgoi, Fredrik Björefors, Kristina Edström, Torbjörn Gustafsson, *Chemistry of Materials* **27**(7), 2591 (2015).
- [9] Yan Xing, Tong Shen, Ting Guo, Xiuli Wang, Xinhui Xia, Changdong Gu, Jiangping Tu, *Journal of Power Sources* **384**, 207 (2018).
- [10] Bing Lu, Bingjie Ma, Xinglan Deng, Bing Wu, Zhenyu Wu, Jing Luo, Xianyou Wang, Gairong Chen, *Chemical Engineering Journal* **351**, 269 (2018).
- [11] Sunghun Choi, Tae-woo Kwon, Ali Coskun, Jang Wook Choi, *Science* **357**(6348), 279 (2017).
- [12] Yoon Hwa, Won-Sik Kim, Byeong-Chul Yu, Seong-Hyeon Hong, Hun-Joon Sohn, *The Journal of Physical Chemistry C* **117**(14), 7013 (2013).
- [13] Leilei Du, Wei Wu, Chao Luo, Huajun Zhao, Dongwei Xu, Ruo Wang, Yonghong Deng, *Solid State Ionics* **319**, 77 (2018).
- [14] Pengfei Gao, Jianwei Fu, Jun Yang, Rongguan Lv, Jiulin Wang, Yanna Nulia, Xiaozhen Tang, *Physical Chemistry Chemical Physics* **11**(47), 11101 (2009).
- [15] Yoshio Masaki, Hongyu Wang, Fukuda, Kenji, Umeno, Tatsuo, Dimov, Nikolay, Ogumi, Zempachi, *Journal of The Electrochemical Society* **149**(12), A1598 (2002).